The memoirs of Faculty of Engineering

Fukuyama University

The 26 th issue, Sep., 2002

Numerical Calculation around Hypersonic/Supersonic Capsule

Hiroaki NAKAMURA*, Shinji SEZAKI*, Keiji MANABE**, and Masatomi NISHIO**

ABSTRACT

The flowfield analysis around a model of re-entry capsule has been carried out utilizing the Finite Element Method (FEM) scheme. In this scheme, the pressure p in the Navier-Stokes equation is expressed by the non-differential form to improve the accuracy in calculation. The propriety of this application was examined by comparing the computational result with the one of Schlieren. In this comparison, the wedge model was used and it was found that they were in good agreement. Subsequently, the flowfield around the capsule was calculated utilizing the FEM scheme. The simulations were carried out under the various Mach number of 10, 5, 3, and 2, respectively. Furthermore, in the case of Mach number of 10, the FEM simulation results such as shock shape, streamline, and vortex region were compared with the experimental ones, which have been carried out by Electric Discharge Method.

Keywords : Supersonic Flow, Hypersonic Flow, Re-entry Capsule, Finite Element Method, and Electric Discharge Method

1. Introduction

The various kinds of studies for space development have been carried out in the world. Especially, the Mars environmental survey program has become more frequent. This program is to rendezvous with an asteroid and to bring back a sample of asteroid soil to Earth. In this mission, the capsule re-enters from the super-orbital flight, so the entering speed of the capsule becomes very high-speed. Therefore, it is important to investigate the flowfield around a capsule. In order to obtain the aerodynamics data around a capsule for the region of supersonic or hypersonic, various kinds of experimental equipment are developed and the theoretical studies or the experimental ones are carried out.[1-8]

In the theoretical studies, the Computational Fluid Dynamics (CFD) technology is useful method for analysis of the flowfield because of the computer development. In this analysis, the Finite Difference Method and the Finite Volume Method are mainly used. However, in the case of Finite Difference Method, it is difficult to give an account of the form of boundary and boundary conditions. Furthermore, the program is dependent on the conditions of flowfield. For the above mentioned reasons, in this study, the flowfield around a capsule was calculated utilizing the FEM scheme.[9], [10] The simulations were carried out under the various Mach number of 10, 5, 3, and 2, respectively. In case of Mach number of 10, the calculated results such as shock shape, streamline, and vortex region were compared with the

* Graduate student, Department of Mechanical Engineering

** Department of Mechanical Engineering

experimental ones, which have been carried out by the Electric Discharge Method.

2. Propriety of Numerical Simulations

In this study, in order to investigate the propriety of FEM, the comparisons of the shock wave over a wedge model between a calculated result and an experimental one by the Schlieren method were carried out. In the numerical calculations, the compressible Navier-Stokes equations were used. The compressible Navier-Stokes equations in conservation form is written as follows:

$$\frac{\partial \mathbf{U}}{\partial t}+\left(\frac{\partial \mathbf{F}_1}{\partial x}+\frac{\partial \mathbf{F}_2}{\partial y}\right)-\left(\frac{\partial \mathbf{G}_1}{\partial x}+\frac{\partial \mathbf{G}_2}{\partial y}\right)=0 \tag{1}$$

where each vector is expressed as follows:

$$\begin{cases} \mathbf{U} = \{\rho \quad \rho u_x \quad \rho u_y \quad \rho e\}^T \\ \mathbf{F}_1 = \mathbf{U}u_x \\ \mathbf{F}_2 = \mathbf{U}u_y \\ \mathbf{G}_1 = \{0 \quad \sigma_{xx} \quad \sigma_{xy} \quad u_x\sigma_{xx}+u_y\sigma_{xy}-q_x\}^T \\ \mathbf{G}_2 = \{0 \quad \sigma_{xy} \quad \sigma_{yy} \quad u_x\sigma_{xy}+u_y\sigma_{yy}-q_y\}^T \end{cases} \tag{2}$$

The notations in Eq.(2) has the following meaning:
ρ =density [kg/m^3], u_x, u_y=velocity components in x and y directions [m/s], e= total energy [J], σ_{xx}, σ_{xy}=stress [Pa], and q_x, q_y=heat flex in x and y directions [J/kg].
In Eq.(2), the stress tensor is consist of the static pressure p and the viscous stress τ and given by

$$\boldsymbol{\sigma} = -p\mathbf{I}+\lambda(\nabla\cdot\mathbf{u})\mathbf{I}+\mu\boldsymbol{\theta} \tag{3}$$

where θ =strain tensor, μ =coefficient of viscosity, λ =second coefficient of viscosity, and I=Kronecker delta. Generally, $\mathbf{F}_1$ and $\mathbf{F}_2$ include the pressure term p. But, in this study, the pressure term p is included in $\mathbf{G}_1$ and $\mathbf{G}_2$ to improve the accuracy in calculation. Furthermore, the coefficient of bulk viscosity μ' is given by

$$\mu' = \lambda+\frac{2}{3}\mu \tag{4}$$

Assuming Stokes Hypothesis of $\lambda = -2/3\,\mu$ Eq.(3) is expressed as follows:

$$\boldsymbol{\sigma} = -p\mathbf{I}-\frac{2}{3}\mu(\nabla\cdot\mathbf{u})\mathbf{I}+\mu\boldsymbol{\theta} \tag{5}$$

In Eq.(5), μ is the coefficient of laminar viscosity and given by the function of temperature. The relation between μ and T is given by Sutherland's equation and they are expressed as follows:

$$\frac{\mu}{\mu_\infty} = \frac{(T_\infty + C_1)}{(T_\infty T^* + C_1)}T^{*3/2} \tag{6}$$

where, $T^*=T/T_\infty$ and $C_1=117$.
In Eq.(1), the equation is not close, so we can not solve the equations. The relations of pressure to other equations of state are needed to solve the equations. The most basic equation of state is a perfect gas. In this study, in order to compare with the experimental results, which obtained by the hypersonic gun tunnel installed in Fukuyama University, the simulations were carried out under the low enthalpy. Therefore, in this study, the gas was assumed to be the perfect gas. In the case of perfect gas, the pressure p is expressed as follows:

$$p = (\gamma-1)\rho\varepsilon \tag{7}$$

where ε =internal energy [J] and γ = ratio of specific heat.

The formulation for FEM is carried out based on the weighted residual method (Galerkin Method). The weighting function w, which takes value 0 on the surface S_U, was considered. We multiply w on Eq.(1) and integrate it over the region A. Eq.(1) becomes as follows:

$$\begin{aligned} \int_A w\frac{\partial \mathbf{U}}{\partial t}dA = &-\int_A w\left(\frac{\partial \mathbf{F}_1}{\partial x}+\frac{\partial \mathbf{F}_2}{\partial y}\right)dA \\ &-\int_A\left(\frac{\partial w}{\partial x}\mathbf{G}_1+\frac{\partial w}{\partial y}\mathbf{G}_2\right)dA \\ &+\int_{Sp} w\bar{P}dS \end{aligned} \tag{8}$$

In order to introduce the upwind effect for the analysis, the SUPG (Streamline Upwind Petrov-Galerkin) method is used. Furthermore, the explicit scheme is used for time integration by making left hand of Eq.(8) diagonal matrix. By this procedure, it does not need to solve the simultaneous equations. Therefore, the calculation time and computer memory can be saved.

The simulation was carried out under the condition that the wedge angle is 20 deg, the Mach number is 10, the freestream density is 4.5×10^{-3} [kg/m^3] , the static pressure is 70 [Pa] and the static temperature is 54 [K] . The computational grid consists of 210×90 nodal points, and non-slip boundary conditions were given for wall surface of the model. Furthermore, the flow is assumed to be a laminar. The computational grid used for calculation and the comparison results are shown in Fig.1 and Fig.2, respectively. In Fig.2, the centerline marks the boundary between a computational result and an experimental result. That is, the upper part of the figure is the computational result and the lower part of the picture is the experimental result. As shown in Fig.2, the shock angle, which obtained by the calculated result was 26.0 ± 0.3 deg and the shock angle, which obtained by the experimental one was 26.2 ± 0.2 deg, respectively. From these results, it was found that they were in good agreement and the propriety of numerical simulations by the FEM was confirmed. Subsequently, the computational results of the flowfield around the capsule are shown.

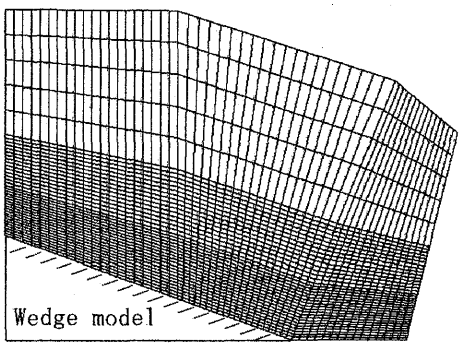

Fig.1 Computational grid around a model.

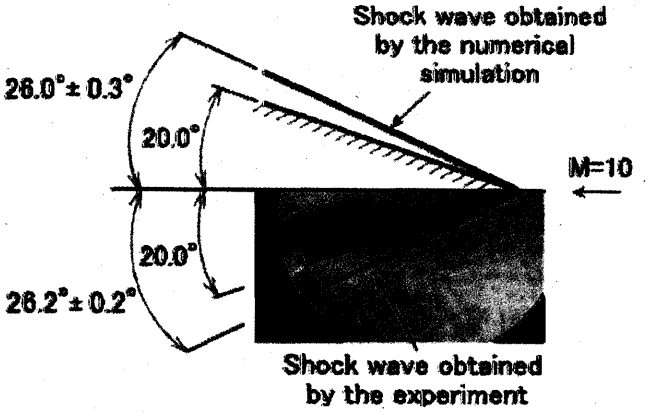

Fig.2 Comparison between the computational result and the experimental result.

3. Simulations by the FEM

3.1 Basic Equations and Computational Method

In the case of axisy mmetric problem, the compressible Navier-Stokes equations in conservation form is as follows:

$$\frac{\partial \mathbf{U}}{\partial t}+\left(\frac{\partial \mathbf{F}_1}{\partial x}+\frac{\partial \mathbf{F}_2}{\partial y}+\underline{\frac{\mathbf{F}_2'}{y}}\right)-\left(\frac{\partial \mathbf{G}_1}{\partial x}+\frac{\partial \mathbf{G}_2}{\partial y}+\underline{\frac{\mathbf{G}_2'}{y}}\right)=0 \qquad (9)$$

where each vector is expressed as follows:

$$\begin{cases}\mathbf{F}_2'=\mathbf{F}_2\\ \mathbf{G}_2'=\{0 \quad \sigma_{xy} \quad \sigma_{yy}-\sigma_\theta \quad u_x\sigma_{xy}+u_y\sigma_{yy}-q_y\}^T\end{cases} \qquad (10)$$

In Eq.(9), the underline shows the term of the axial symmetry.

As a boundary conditions, they are based on the relations:

$$\mathbf{U}=\bar{\mathbf{U}} \ (\text{on } S_U), \quad \mathbf{G}_1 n_x+\mathbf{G}_2 n_y=\bar{P} \ (\text{on } S_P) \qquad (11)$$

where $\bar{\mathbf{U}}$ =the known quantities and S=on boundary.

The weighted function w, which takes value 0 on the surface S_U, was considered. We multiply w on Eq.(11) and integrate it over the region A. Eq.(11) becomes as follows:

Table 1 Freestream conditions

Case	V_∞ [m/s]	M_∞	P_∞ [Pa]	T_∞ [K]	ρ_∞ [kg/m^3]	Re *	γ
1	1500	10.0	70.0	54.0	4.5×10^{-3}	1.95×10^{6}	1.4
2	1500	5.0	1197.0	226.5	1.8×10^{-2}	1.86×10^{6}	1.4
3	895	3.0	2549.0	221.6	4.0×10^{-2}	2.52×10^{6}	1.4
4	590	2.0	5529.0	216.7	8.9×10^{-2}	3.78×10^{6}	1.4

* The values of per meter

$$2\pi\int_A w\frac{\partial \mathbf{U}}{\partial t}dA=-2\pi\int_A w\left(\frac{\partial \mathbf{F}_1}{\partial x}+\frac{\partial \mathbf{F}_2}{\partial y}\right)ydA$$
$$-2\pi\int_A\left(\frac{\partial w}{\partial x}\mathbf{G}_1+\frac{\partial w}{\partial y}\mathbf{G}_2\right)ydA$$
$$+2\pi\int_{Sp}w\bar{P}ydS$$
$$-2\pi\int_A w\left(\frac{F_2'}{y}-\frac{G_2'-G_2}{\underline{y}}\right)ydA \qquad (12)$$

3.2 The Conditions of Calculation

The flowfield analysis around the capsule was calculated by the FEM. In this study, the simulations were carried out under the various Mach number of 10, 5, 3, and 2, respectively. The freestream conditions used for calculation are shown in Table.1. In Table 1, the case 1 is the physics quantities for the experiment and the other cases are the physics quantities for the standard atmosphere. Figure 3 shows the model dimensions of capsule, which used for simulations. In these simulations, the computational grid consists of 194× 100 nodal points, and non-slip boundary conditions were given for wall surface of the model. The computational grid used for calculation is shown in Fig.4.

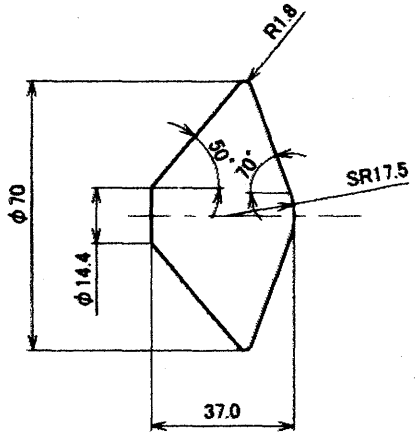

Fig.3 Model dimensions of capsule.

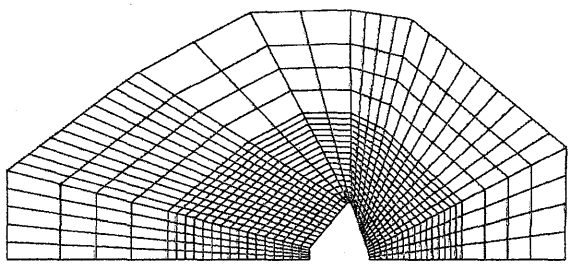

Fig.4 Computational grid around a model.

4. Computational Results and Discussions

The flowfield around the capsule such as shock waves, velocity vectors, and streamlines were calculated under the various Mach number of 10, 5, 3, and 2, respectively. In the case of M=10, the shock wave around the capsule which obtained by the Electric Discharge Method are shown in Fig.5. Figure 6 shows the streamlines and the density distributions around the capsule, which obtained by the FEM. Furthermore, Figs. 7 and 8 shows the comparison between the computational results and the experimental ones. In Fig.7, the solid line expresses the streamline, which obtained by the FEM and the dotted line expresses the streamlines and the shock wave, which obtained by the Electric Discharge Method. Fig.8 shows the shock wave around the capsule, which obtained by the FEM and the Schlieren Method. In this case, the upper part of the figure is the computational result and the lower part of the figure is the experimental result. From these comparisons, a good correlation between them was found.

Next, the density distributions around the capsule are shown in Fig.9. In this case, the shock waves are expressed by the density ratio, i.e. ρ/ρ_∞=the density for downstream of the shock wave / the density for upstream of the shock wave. From Fig.9, it is found that the largest shock standoff distance occurs with the M=2. Furthermore, at the shoulder of capsule, the decreases of

density ratio were confirmed in the downstream directions. This phenomenon is concerned with the expansion waves at the shoulder of capsule. Therefore, the directions of flow are change and it flows along the wall of capsule when it across the expansion waves. In order to examine these phenomena, the velocity vectors and the streamlines around the capsule were calculated. The results are shown in Figs.10 and 11, respectively. In Figs.10 and 11, it was found that there were the vortex exists in the wake. From these computational results, it was found that the separation points were almost the same, but in the downstream directions, the location of the wake stagnation point for M=10 was larger than that of the M=2.

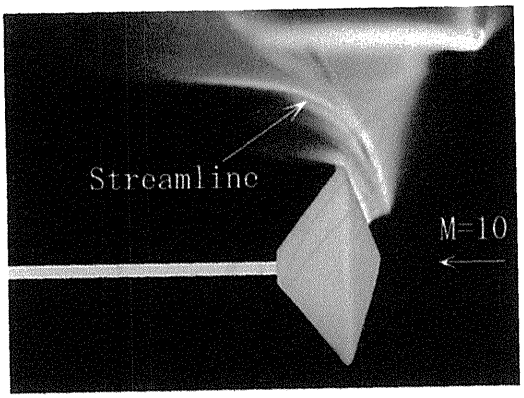

(a)

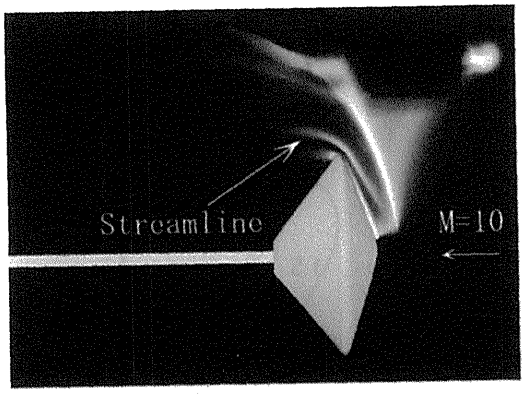

(b)

Fig.5 Visualization of the streamline by the Electric Discharge Method. (M=10)

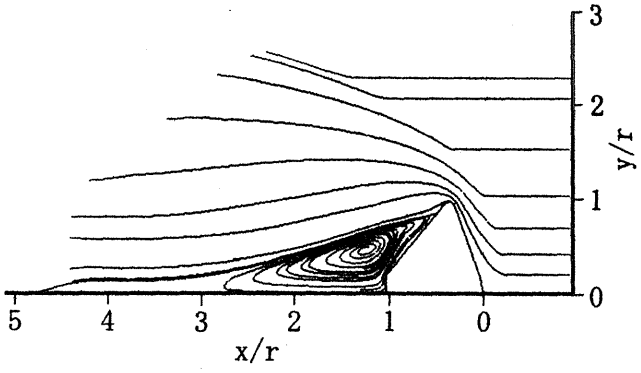

(a) Calculated streamline around the capsule.

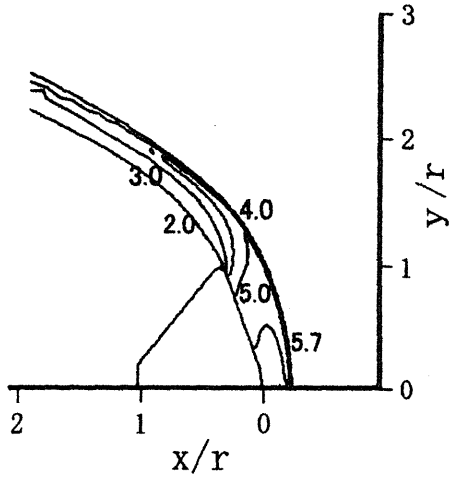

(b) Calculated density distribution around the capsule. (max ρ / ρ_∞=5.7)

Fig.6 Flowfield around the capsule. (M=10)

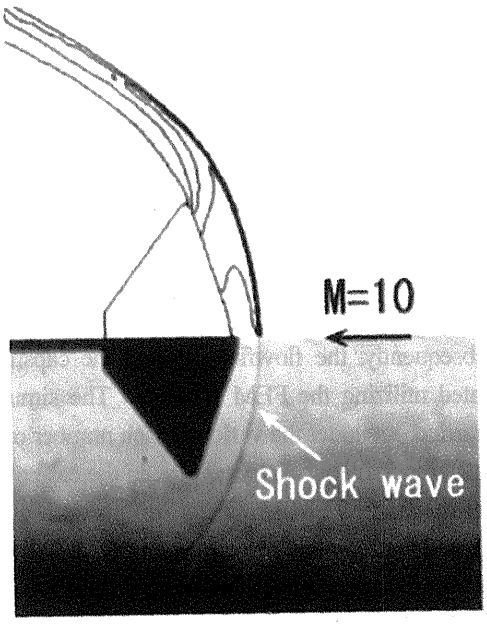

Fig.8 Comparison between the computational result and the experimental result. (M=10)

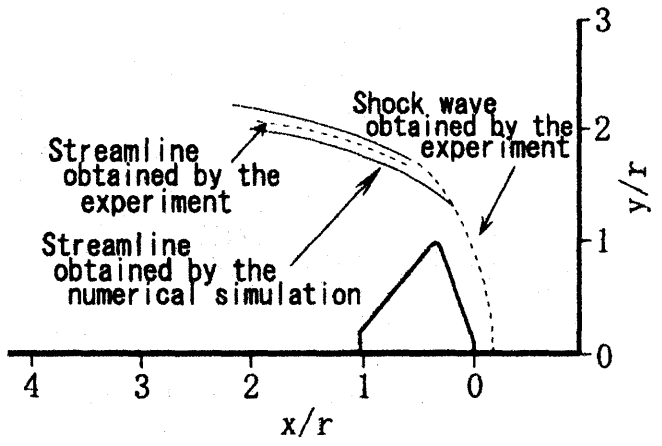

(a)

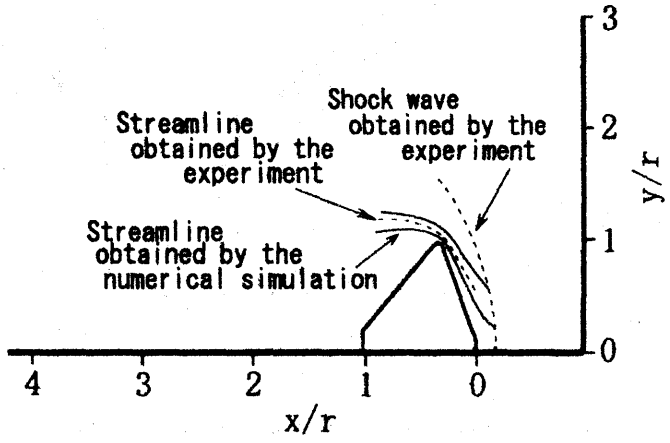

(b)

Fig.7 Comparison between the computational result and the experimental result. (M=10)

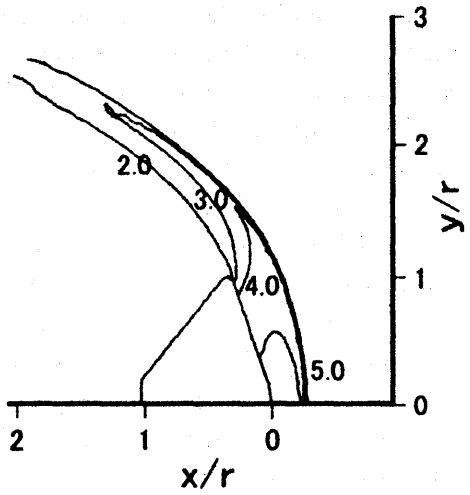

(a) M=5, max ρ / ρ_∞=5.0

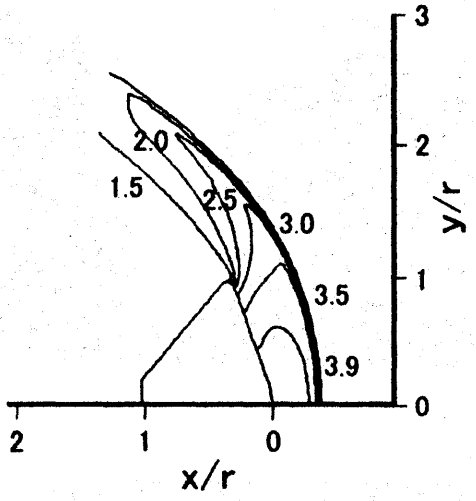

(b) M=3, max ρ / ρ_∞=3.9

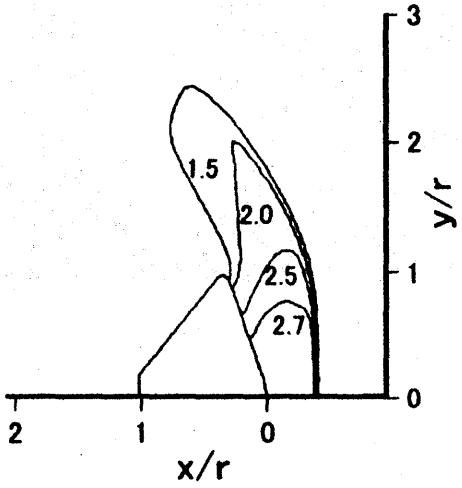

(c) M=2, max ρ / ρ_∞=2.7

Fig.9 Nondimensional density.

5. Conclusions

In this study, the flowfield around the capsule were calculated utilizing the FEM. First, in order to investigate the propriety of FEM, the comparisons of the shock wave over a wedge model between the calculated result and the experimental one by the Schlieren method were carried out.

Subsequently, the flowfield around the capsule was calculated utilizing the FEM scheme. The simulations were carried out under the various Mach number of 10, 5, 3, and 2, respectively. Furthermore, in the case of Mach number of 10, the FEM simulation results such as shock wave and streamline were compared with the experimental ones, which have been carried out by Electric Discharge Method. From these comparisons, it was found that they were in good agreement.

Furthermore, In this study, in order to compare with

the experimental results, which obtained by the hypersonic gun tunnel installed in Fukuyama University, the simulations were carried out under the low enthalpy.

References

[1] Virendra K.Dogra, James N.Moss and Joseph M.Price.:Near-Wake Structure for a Generic Configuration of Aeroassisted Space Transfer Vehicles, J.Spacecraft Rockets., **31** (1994), pp.953-959.

[2] M.S.Kim, J.M.Loellbach, and K.D.Lee.:Effects of Gas Models on Hypersonic Base Flow Calculations, J.Spacecraet Rockets., **31** (1994), pp.223-230.

[3] Virenda K.Dogra, Jeff C.Taylor and H.A.Hassan.:Effects of Chemistry on Blunt-Body Wake Structure, AIAA J., **33** (1995), pp.463-469.

[4] Moss, J.N., Mitcheltree, R.A., Dogra, V.K., and Wilmoth, R.G.:Hypersonic Blunt-Body Wake Computations Using DSMC and Navier-Stokes Solvers, AIAA Paper 93-2807, 1993.

[5] Olynick, D.R., Taylor, J.C., and Hassan, H.A.:Comparisons Between DSMC and the Navier-Stokes Equations for Re-entry Flows, AIAA Paper 93-2810, 1993.

[6] Nishio, M.:Qualitative Model for Visualizing Shock Shapes, AIAA J., **30** (1992), pp.2246-2248.

[7] Nishio, M.:Method for Visualizing Streamline Around Hypersonic Vehicles by Using Electric Discharge, AIAA J., **30** (1992), pp.1662-1663.

[8] Sezaki, S., Nakamura, H., and Nishio, M.:Visualization of Flowfield Around Hypersonic Re-entry Capsule Using Electric Discharge Method, The 10th International Symposium on Flow Visualization, Kyoto, Japan, 2002, F0182.

[9] O.C.Zienkiewicz, J.Szmelter and J.Peraire.:Compressible and incompressible flows; An algorithm for all seasons, Comput.Methods.Appl.Mech.Engrg., **78**, (1990), pp.105-121.

[10] P.Arminjon and A.Dervieux.:Construction of TVD-like Artificial Viscosities on two-dimensional arbitrary FEM grids, J.Comp.Physics., **106** (1993), pp.176-198.

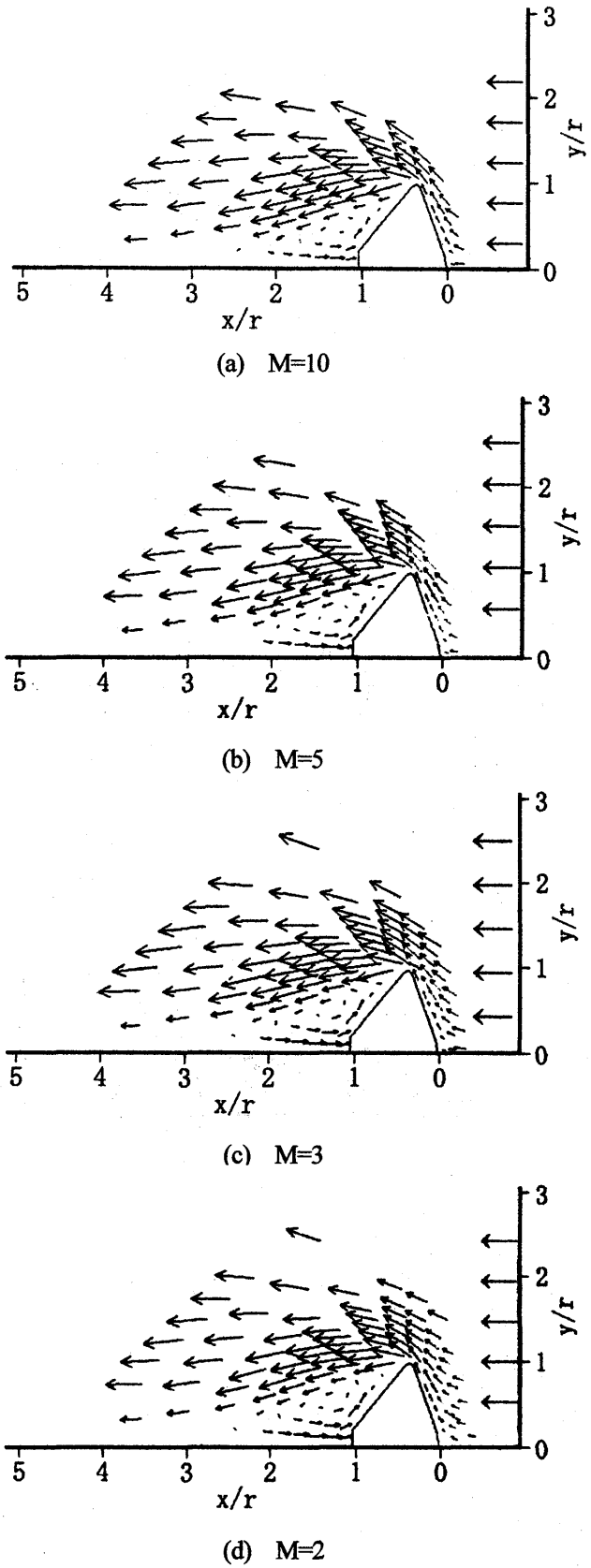

(a) M=10

(b) M=5

(c) M=3

(d) M=2

Fig.10 Calculated velocity field around the capsule.

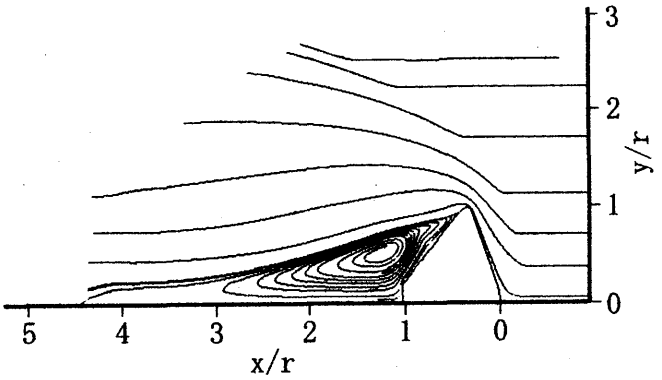

(a) M=5

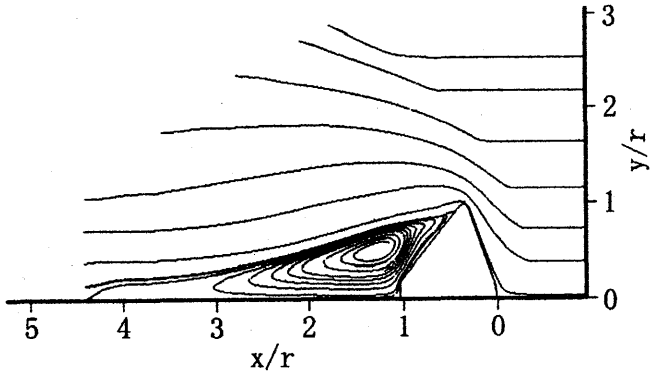

(b) M=3

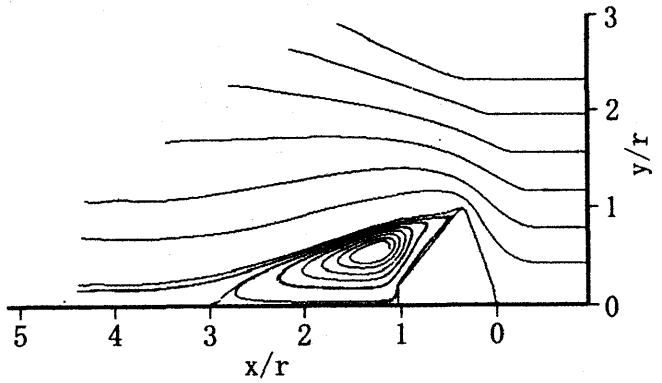

(c) M=2

Fig.11 Calculated streamline around the capsule.